

POLY(ESTER AMIDE)/CLAY NANOCOMPOSITES PREPARED BY IN SITU POLYMERIZATION OF THE SODIUM SALT OF N-CHLOROACETYL-6-AMINOHEXANOIC ACID



Laura Morales,^{1,2} Lourdes Franco,^{1,2} María Teresa Casas,¹ Jordi Puiggalí ^{1,2}

¹Departament d'Enginyeria Química, Universitat Politècnica de Catalunya, Av. Diagonal 647, E-08028, Barcelona, SPAIN

²Centre de Recerca en NanoEnginyeria (CRNE), Universitat Politècnica de Catalunya, Edifici C', c/ Pascual i Vila s/n, E-08028, Barcelona, SPAIN

INTRODUCTION

Preparation of polymer nanocomposites is nowadays an important research subject since polymer properties can be enhanced and their range of applications extended by using molecular or nanoscale reinforcements rather than conventional fillers. Poly(ester amide)s constitute a promising family of materials with some advantages associated with the hydrophilic character of their amide groups and the ability to establish strong hydrogen bond interactions that may influence both thermal and mechanical properties. Furthermore, the presence of ester groups should ensure degradability, although at a lower rate than in parent polyesters. C25A organo-modified montmorillonite has proved to be effective for the preparation of nanocomposites from the degradable alternating poly(ester amide) constituted by glycolic acid and 6-aminohexanoic acid units (poly(glc-*alt*-amh)) by the in situ polymerization technique.

MELT CRYSTALLIZATION OF THE NEAT POLY(ESTER AMIDE) AND ITS NANOCOMPOSITE WITH C25A

The spherulite radial growth rates (*G*) of the neat poly(glc-*alt*-amh) sample and its nanocomposite with C25A were determined by means of the evolution of the spherulite radius versus time (Figure 3a).

Optical micrographs (Figures 3b and 3c) revealed that the nucleation density diminished in the nanocomposite. Thus, a decrease in the overall crystallization rate of the nanocomposite can be inferred considering both, primary nucleation and crystal growth rate. This feature has been reported for nanocomposites of materials characterized by an exfoliated structure.

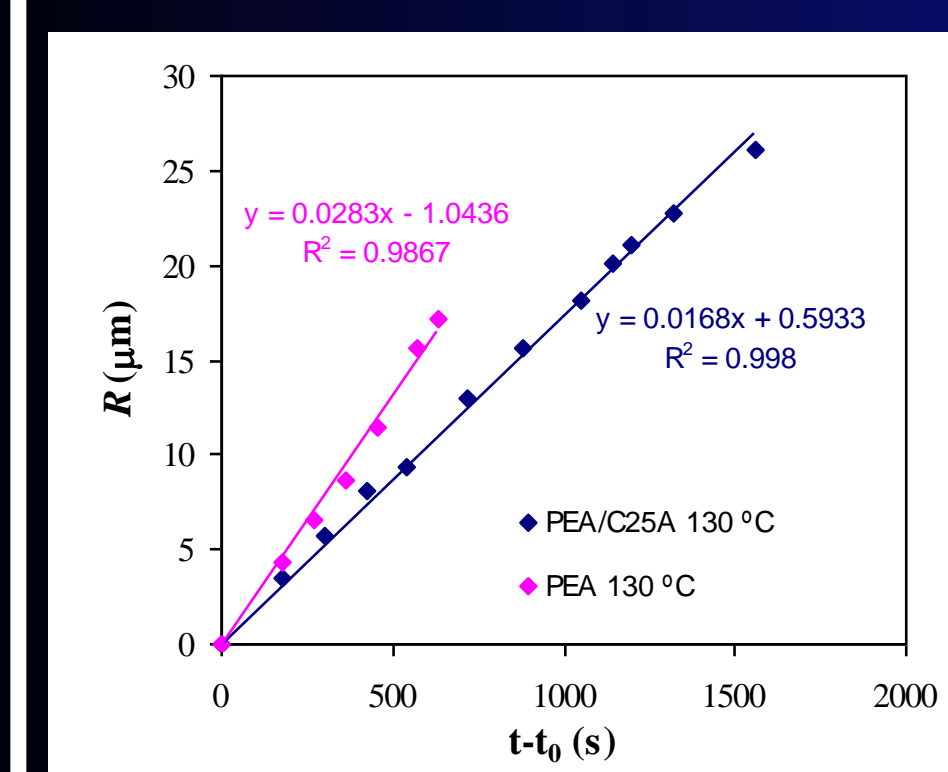


Figure 3a. Plot of the radius of spherulites of the neat polymer and its nanocomposite with C25A versus crystallization time for an isothermal crystallization temperature of 130 °C.

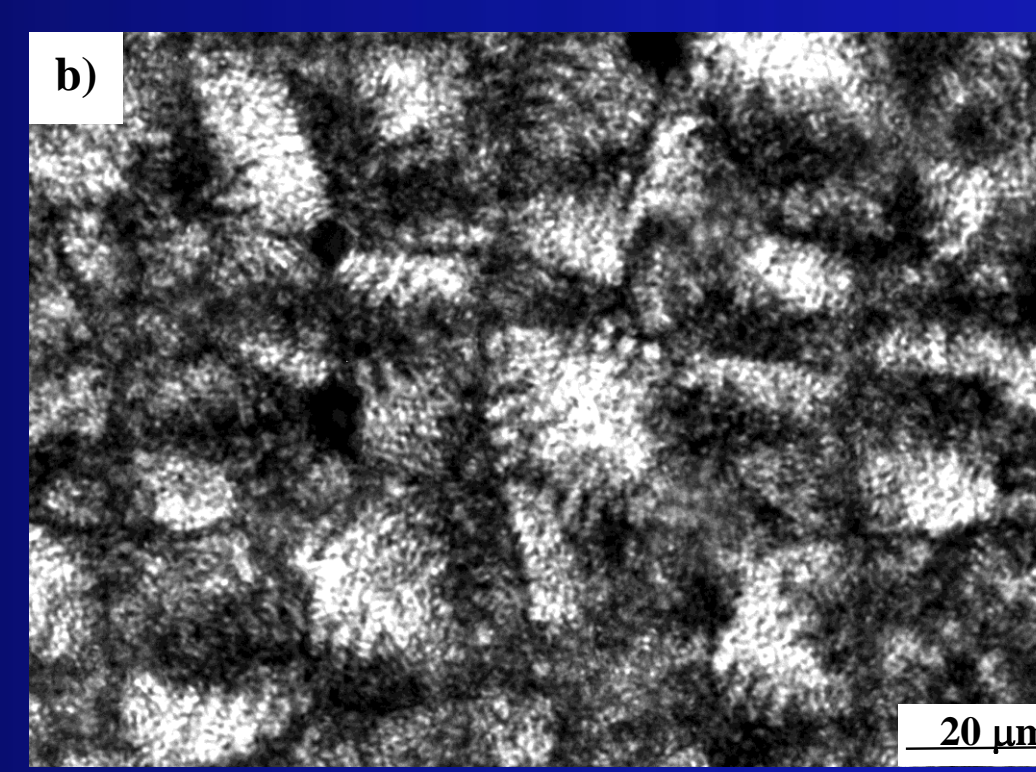


Figure 3b. Polarized optical micrograph showing spherulites of the neat poly(glc-*alt*-amh) sample crystallized at 130 °C.

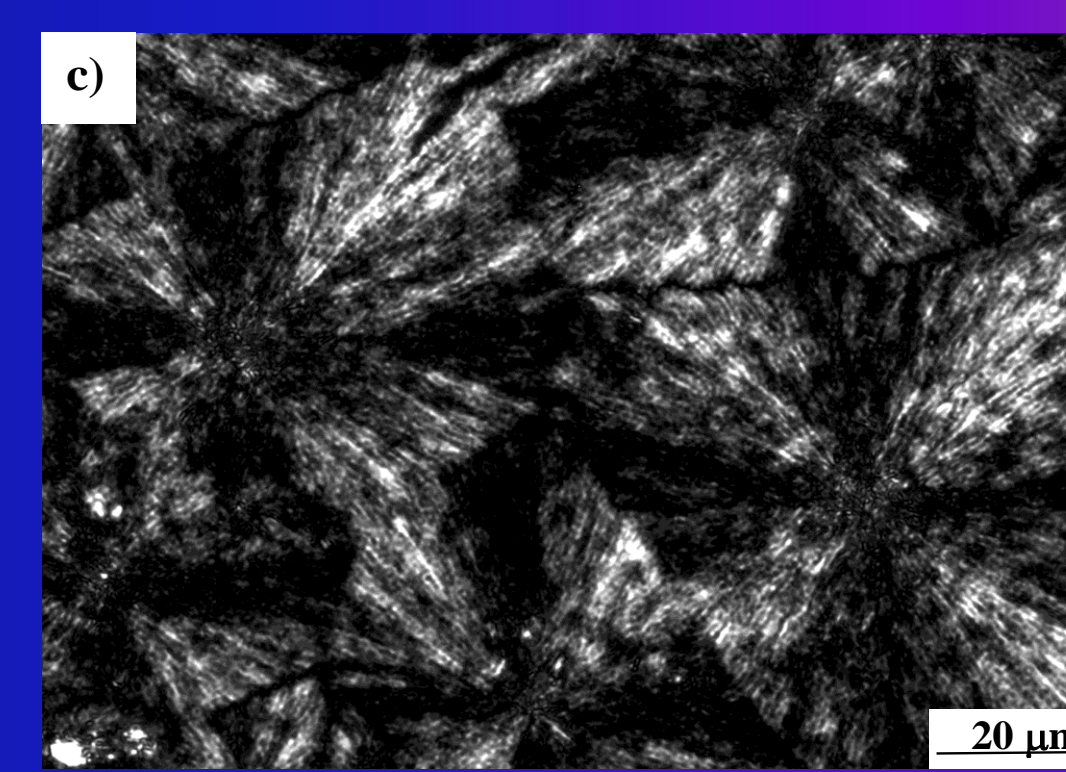


Figure 3c. Polarized optical micrograph showing spherulites of the poly(glc-*alt*-amh) nanocomposite with C25A crystallized at 130 °C.

NONISOTHERMAL POLYMERIZATION STUDY

Synchrotron experiments were performed to gain insight the nonisothermal polymerization process (Figure 4). X-ray profiles clearly showed that all diffraction peaks were shifted to lower angles when temperature was increased, as expected from the thermal expansion of the unit cell. The profiles showed two peaks at $2\theta \sim 19$ and 22° corresponding to the (100) and (110) reflections of the NaCl structure (~ 0.326 and 0.282 nm, respectively) and different peaks in the 14 - 17° 2θ range corresponding to the monomer structure. The intensity of the NaCl peaks started to increase and, at the same time, the monomer peaks gradually became weaker. Finally, an amorphous halo and small peaks attributed to (*hk*0) reflections of the clay were observed when temperature reached a value close to 190 °C. The polymerization finished in an amorphous or liquefied state since at this temperature the intensity of NaCl did not reach the asymptotic value that corresponds to the maximum amount of NaCl that could be formed.

X-ray diffraction patterns taken during a subsequent cooling run (Figure 5) revealed that polymerization was successful since the characteristic diffraction peaks of poly(glc-*alt*-amh) appeared progressively.

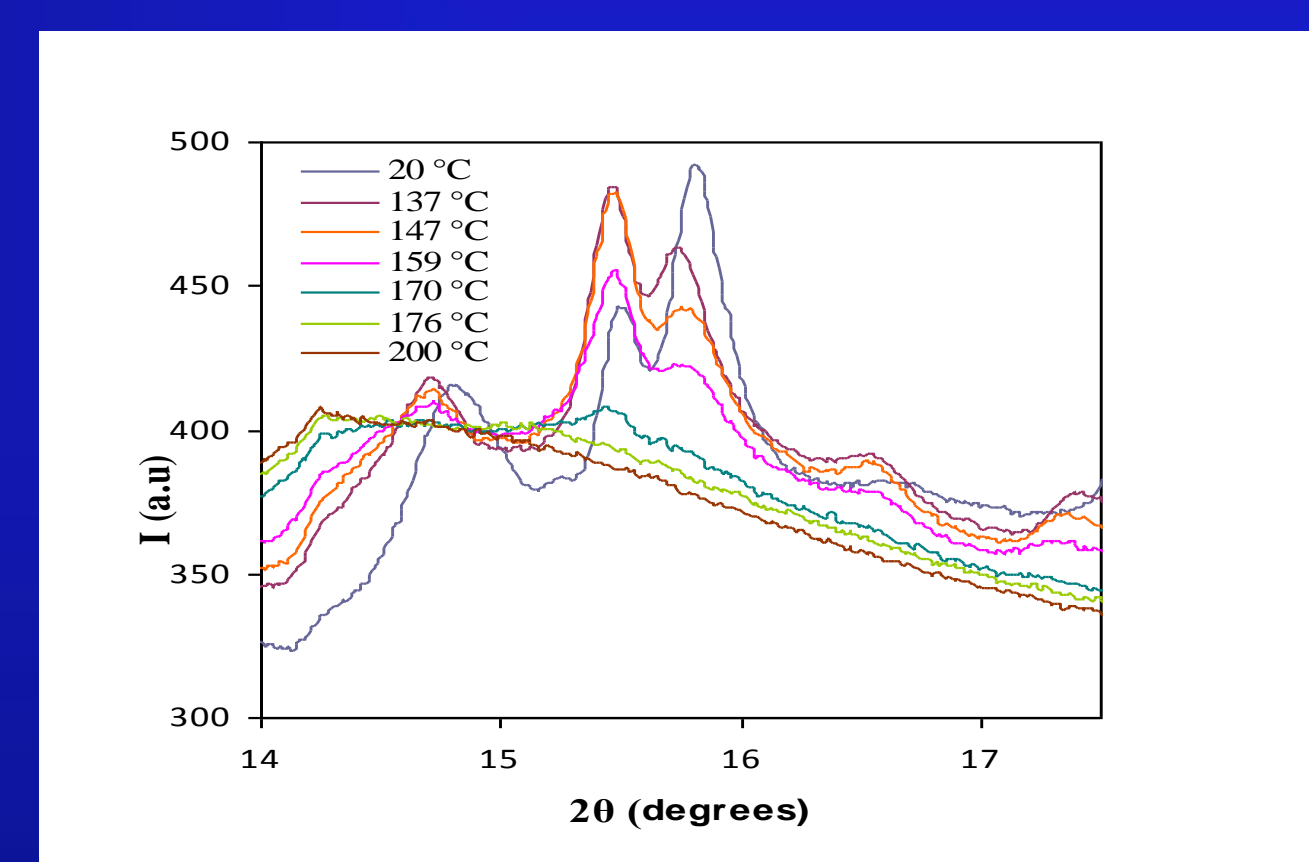


Figure 4. WAXD profiles taken during the nonisothermal polymerization performed at a heating rate of 20 °C/min with the monomer / C25A mixture

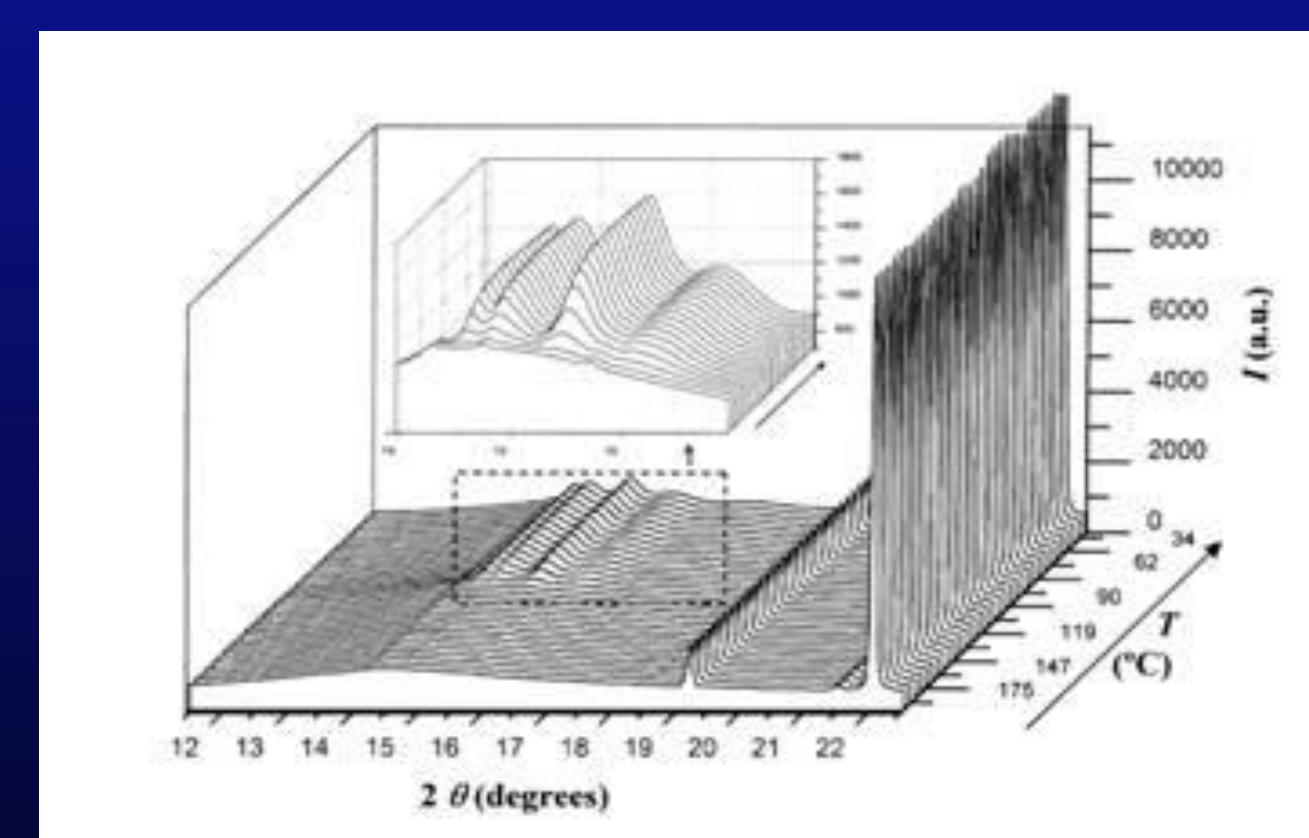
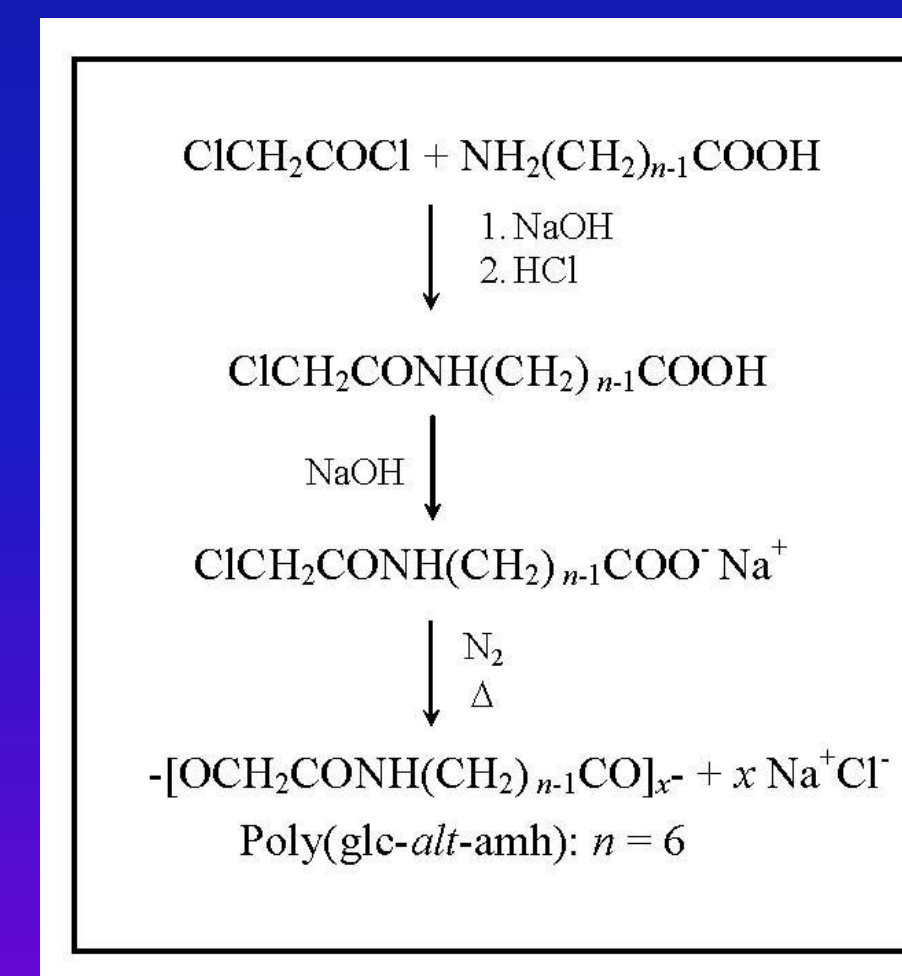


Figure 5. WAXD profiles taken during the nonisothermal crystallization that occurred during a cooling run performed at 20 °C/min of a nonisothermally polymerized monomer / C25A mixture at a heating run of 20 °C/min.

PREPARATION OF NANOCOMPOSITES

The monomer, sodium chloroacetylaminohexanoate, was synthesized following the Scheme 1. Polymerization was carried out by heating the monomer / clay mixture to 160°C. Five different layered phyllosilicates (Table 1) were investigated, obtaining the most interesting result with Cloisite 25A. X-ray diffraction patterns (Figure 1) indicated that the characteristic interlayer peak of the silicate structure was absent in the nanocomposite. Transmission electron micrographs (Figure 2) clearly showed that an intercalated structure was predominant, varying the interlayer spacings from 1.4 to 3.2 nm. This seemed as a first step towards a fully exfoliated structure.



Scheme 1. Synthesis of poly(ester amide)

Clay Type	Chemical Structure of Organic Modifier
NanoFl 757	Natural Montmorillonite (Na ⁺)
NanoFl 848	$\begin{array}{c} \text{C}_6\text{H}_{13} \\ \\ \text{H}-\text{N}-\text{H} \\ \\ \text{H} \end{array}$
Cloisite 30B	$\begin{array}{c} \text{H}_3\text{C}-\text{N}-\text{CH}_2\text{CH}_2\text{OH} \\ \\ \text{CH}_2\text{CH}_2\text{OH} \end{array}$
Cloisite 20A	$\begin{array}{c} \text{H}_3\text{C}-\text{N}-\text{CH}_3 \\ \\ \text{H} \end{array}$
Cloisite 25A	$\begin{array}{c} \text{CH}_3 \\ \\ \text{H}_3\text{C}-\text{N}-\text{CH}_2\text{CH}_2\text{CH}_2\text{CH}_2\text{CH}_2\text{CH}_3 \\ \\ \text{H} \end{array}$

Table 1. Characteristic of organoclays

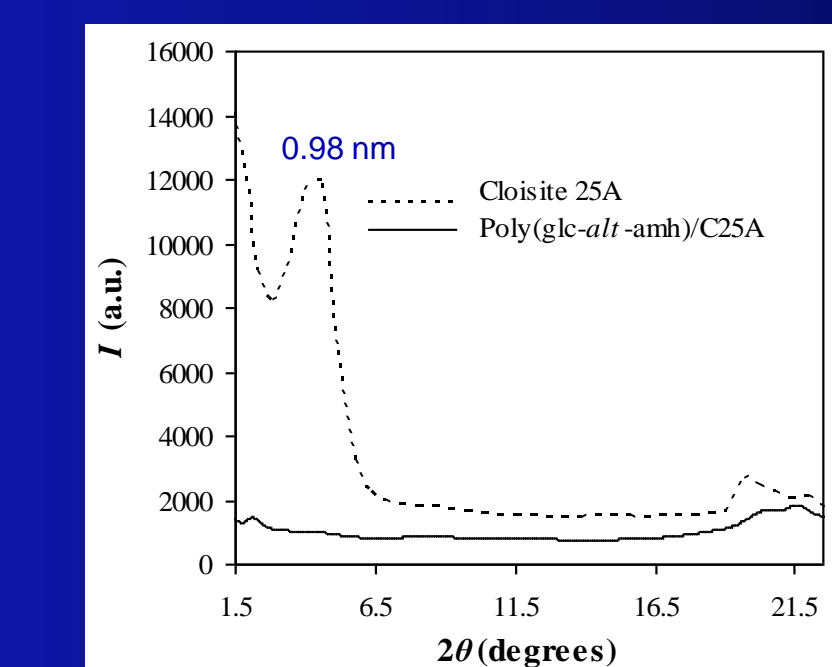


Figure 1. X-ray diffraction patterns of neat Cloisite 25A (dotted line) and the nanocomposite obtained by in situ polymerization of N-chloroacetyl-6-aminohexanoic acid with 3% clay content (solid line).

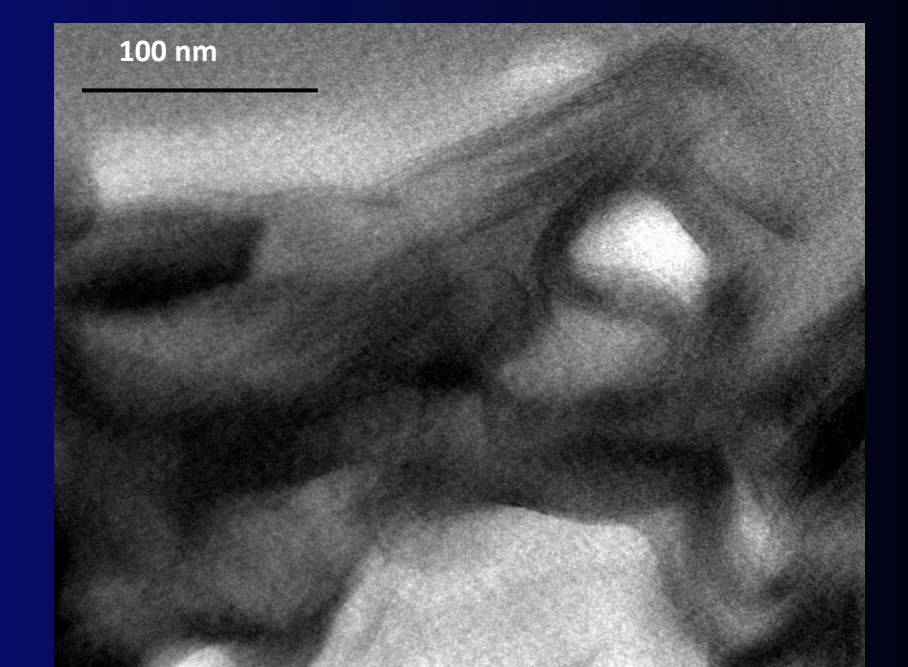


Figure 2. Transmission electron micrograph showing the morphology of the nanocomposite obtained by in situ polymerization of N-chloroacetyl-6-aminohexanoic acid in the presence of 3% clay content.

ISOTHERMAL POLYMERIZATION STUDY

For all assayed temperatures the polymerization process of the neat monomer was faster than for its nanocomposite with C25A. Polymerization kinetics was evaluated by both, WAXD and FTIR experiments following the diffraction intensity of the (110) NaCl reflection or the time evolution of the 1741 cm^{-1} absorption band of the ester group, respectively (Figures 6 and 7). The activation energy and the frequency factor for the polymerization were derived by assuming an Arrhenius-type dependence on temperature for the kinetic constant (Figure 8).

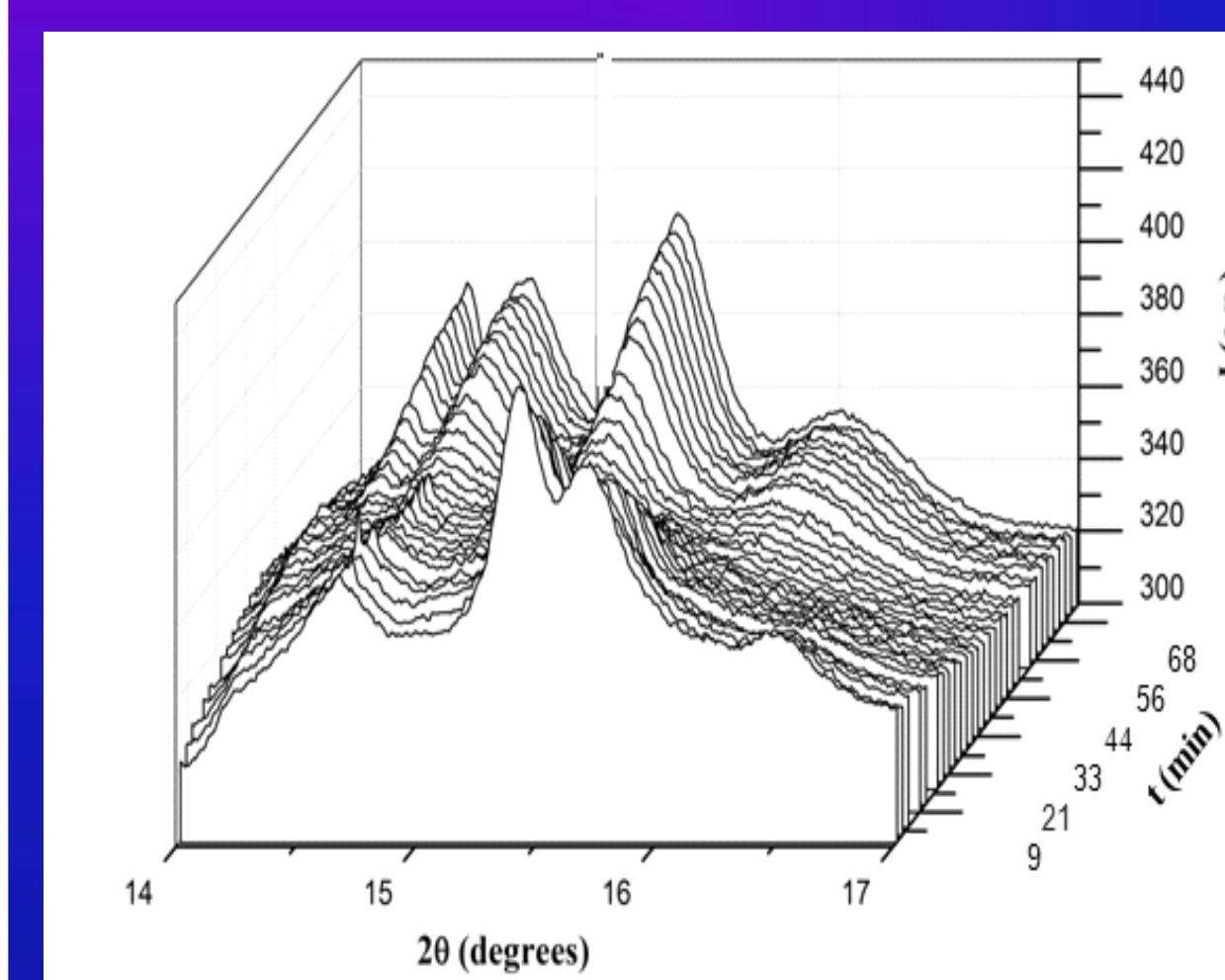


Figure 6a. WAXD profiles taken during the isothermal polymerization of the monomer / C25A mixture performed at 125 °C.

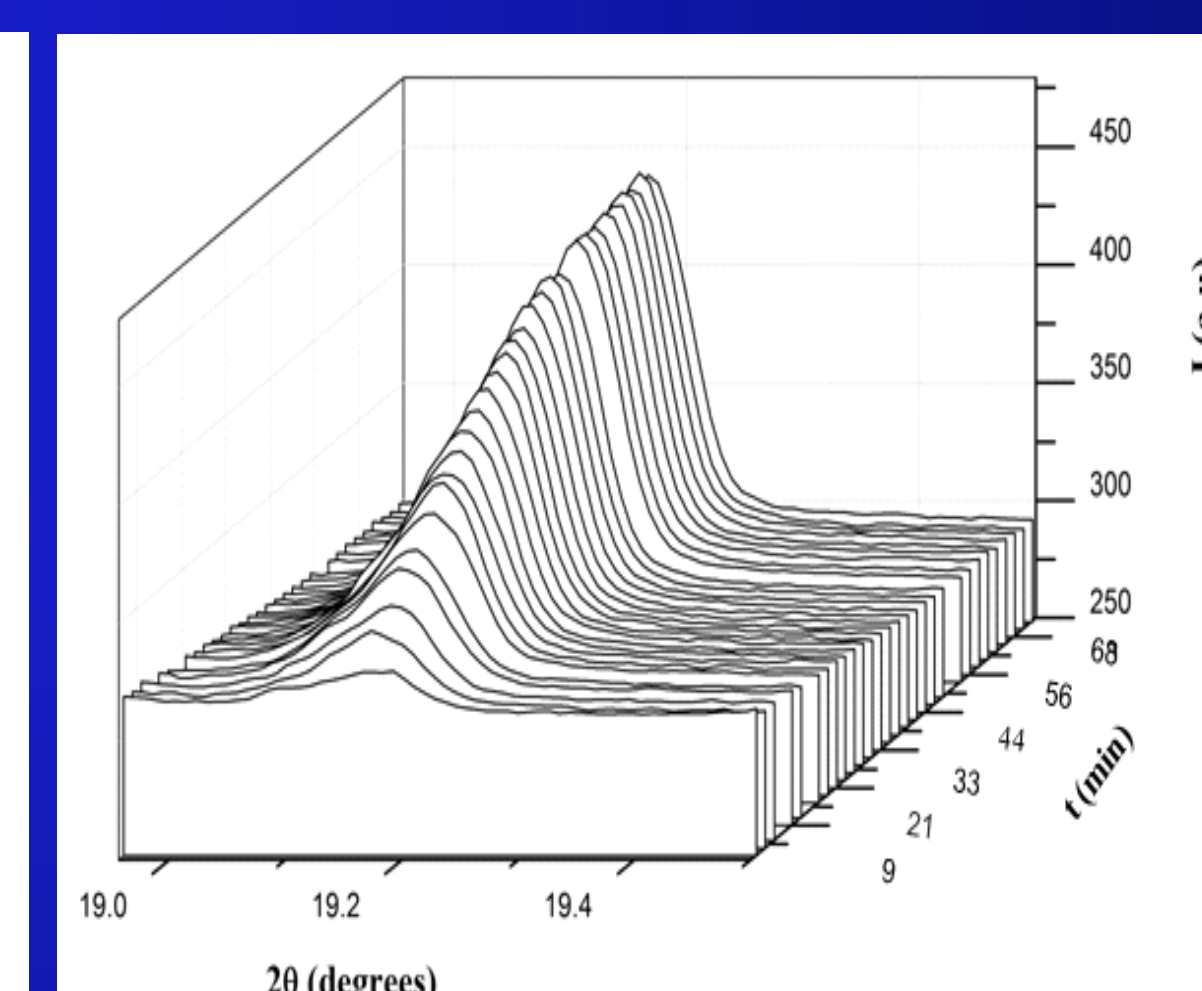


Figure 6b. WAXD profiles taken during the isothermal polymerization of the monomer / C25A mixture performed at 125 °C. The evolution of the weak NaCl reflection at $2\theta \approx 19^\circ$ is shown.

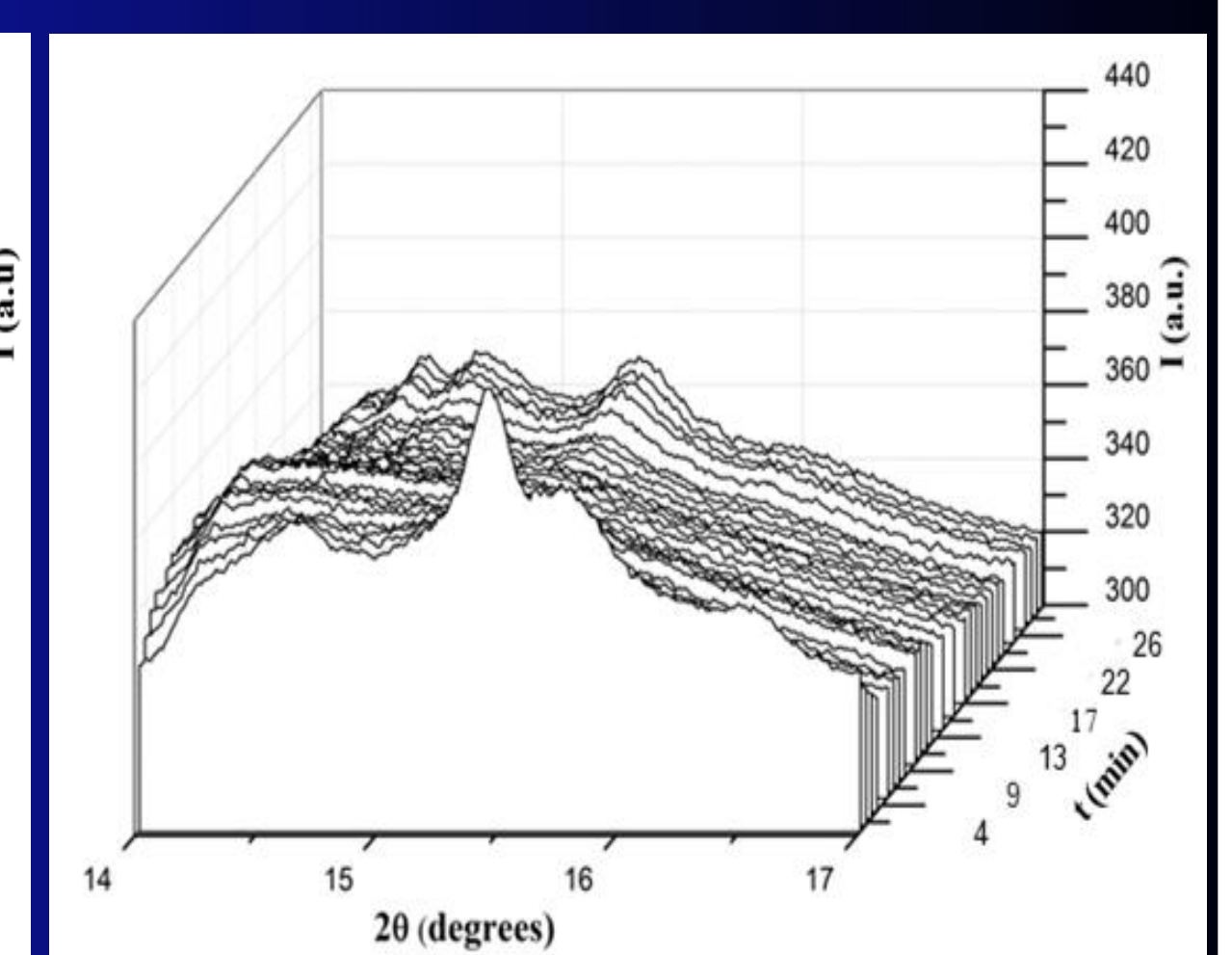


Figure 6c. WAXD profiles taken during the isothermal polymerization of the monomer / C25A mixture performed at 145 °C.

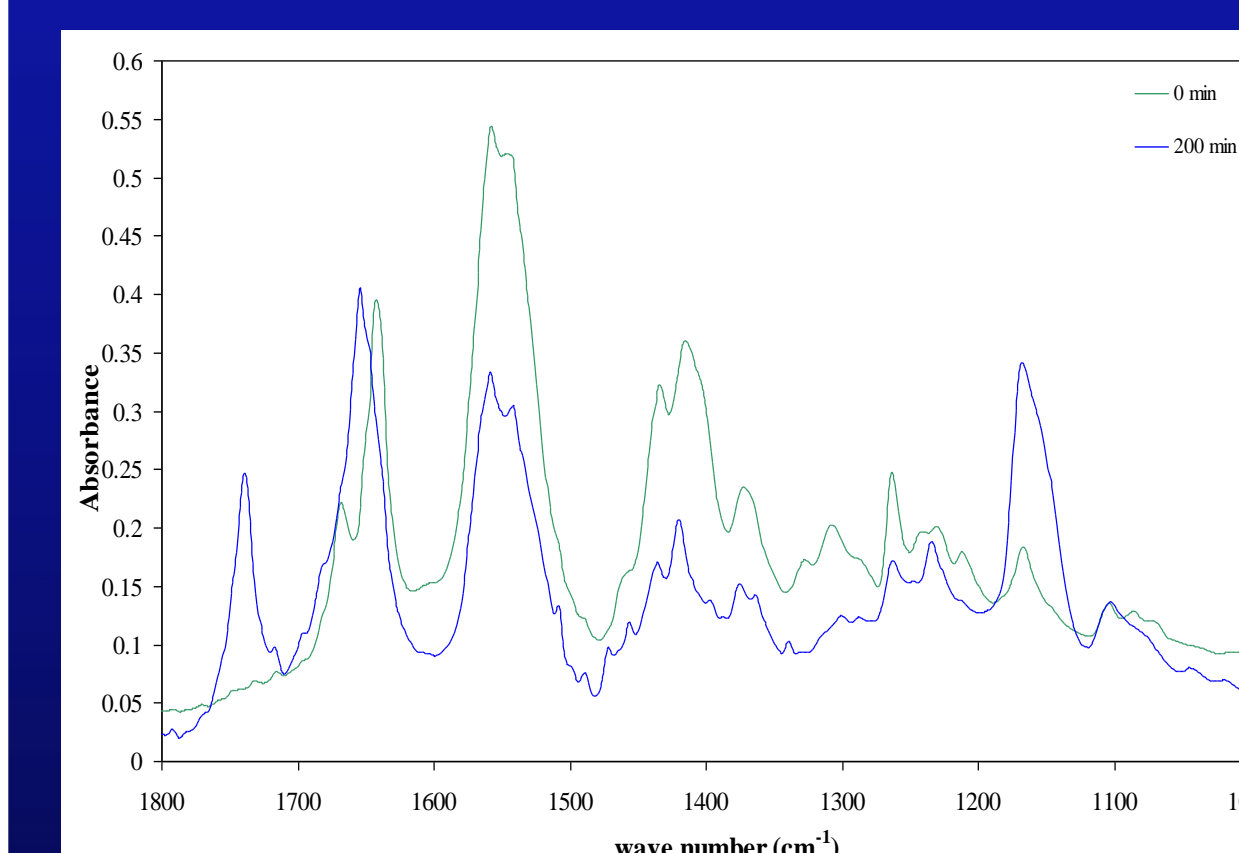


Figure 7a. Absorbance FTIR spectra (1800 - 1000 cm^{-1}) at the beginning and at the end of the polymerization reaction performed at 100 °C with the monomer / C25A mixture.

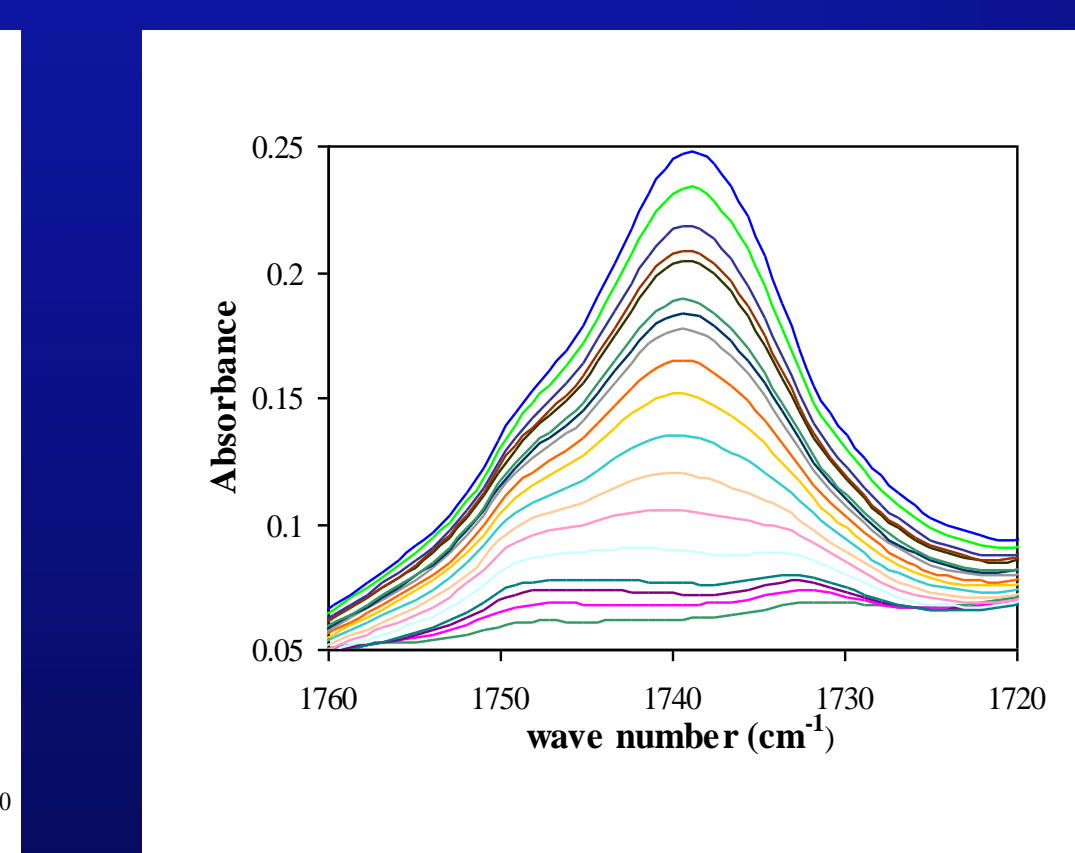


Figure 7b. Evolution of the band associated with the carboxylic ester group (1741 cm^{-1}) for a polymerization performed at 100 °C with the monomer / C25A mixture.

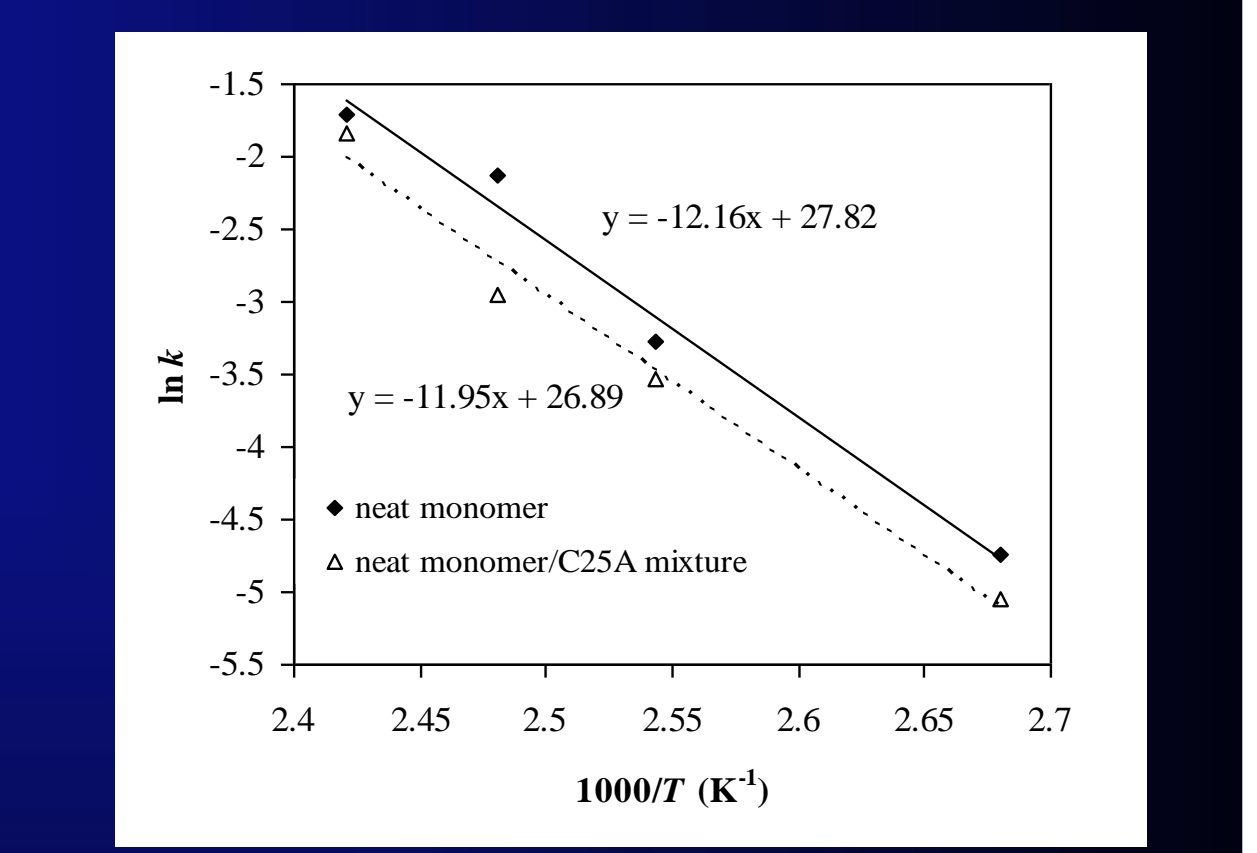


Figure 8. Plot of $\ln k$ versus the reciprocal of the polymerization temperature for the neat monomer and the monomer/C25A mixture.

CONCLUSIONS

- C25A organo-modified montmorillonite has proved to be effective for the preparation of nanocomposites of the degradable alternating poly(ester amide) constituted by glycolic acid and 6-aminohexanoic acid units by the in situ polymerization technique.
- The temperature dependence of the polymerization kinetic constant allowed inferring that kinetic differences between the polymerization of the neat monomer and its mixture with C25A could be attributed to the preexponential frequency factor.